JOURNAL OF SOLID STATE CHEMISTRY 42, 107–119 (1982)

Enhanced Ionic Conduction in Dispersed Solid Electrolyte Systems (DSES) and/or Multiphase Systems: AgI–Al_2O_3, AgI–SiO_2, AgI–Fly ash, and AgI–AgBr

K. SHAHI AND J. B. WAGNER, JR.

Center for Solid State Science and Department of Physics, Arizona State University, Tempe, Arizona 85287

Received March 20, 1981; in revised form December 8, 1981

Alternating current electrical conductivity (σ) data are presented for AgI–Al_2O_3, AgI–SiO_2, AgI–fly ash, and AgI–AgBr as functions of composition, temperature, and frequency. Unlike the predictions of the classical theories of Rayleigh and Maxwell, conductivity enhancements by as much as two to three orders of magnitude have been obtained at 25°C without appreciable change in the electronic conductivities. The σ enhancement strongly depends on the particle size and the concentration of the dispersoids, as well as on the process variables, e.g., the heat treatment of the dispersoids, premelting of the electrolytes, etc., and also on cold and hot pressing. The Al_2O_3 is found somewhat unique in the sense that it leads to a maximum enhancement (by $\sim 10^3$ times) when used as received and when the electrolyte in the mixture is premelted, while SiO_2 and fly ash (without premelting the electrolyte) lead to an enhancement by a factor of ~50 and show no significant effect of premelting. SEM studies, coupled with the frequency-dependent σ data, suggest that the enhancement is due to bulk rather than grain-boundary or surface conduction. The enhanced σ is usually accompanied by a decrease in activation energy, suggesting that the dispersoids generate excess of lattice defects and thereby increase the conductivity, which is consistent with a recent theoretical model, as well as with the latest thermoelectric power measurements.

Introduction

Solid electrolytes (*1*, *2*) characterized by exceptionally high ionic conductivity and relatively small electronic conductivity have attracted a great deal of attention because of their unique transport properties and potential applications in batteries, sensors, etc. While intensive researches in the past decade have already resulted in a number of good solid electrolyte materials, efforts continue in discovering new materials and methods for increasing the level of ionic conduction. The various techniques employed thus far to enhance the ionic conductivity include the addition of aliovalent impurities (e.g., $CaO \cdot ZrO_2$), the stabilization of unique open-channel (*3*, *4*) structures (e.g., $RbAg_4I_5$, Na–β–Al_2O_3, etc.), and disordered glassy phases (*5*).

A number of investigations (*6–10*) have recently reported significant enhancement in ionic conductivity by the dispersion of fine, insulating and insoluble Al_2O_3 particles and, more importantly, without altering the electronic conductivity appreciably. These so-called dispersed solid electrolyte systems (DSES) have become increasingly important to both experimentalists (*6–9*) and theorists (*7*, *11*). Much of the previous work, with one exception (*10*) that deals with the dispersion of SiO_2 in LiI, is limited

0022-4596/82/050107-13$02.00/0

to dispersion of Al_2O_3 in a number of solid electrolytes, such as LiI, AgI, CuCl, etc. In this paper we report the electrical transport data on AgI containing a variety of dispersions, namely, the previously reported systems AgI–Al_2O_3 (*8*) and AgI–AgBr (two-phase) (*12*) and the newly investigated systems AgI–fly ash and AgI–SiO_2 (*13*). A comparison of these four systems then reveals that the two-phase mixtures and/or DSES in general exhibit a higher conductivity than that of starting materials.

Experimental

(*i*) *Origin of the Chemicals*

High-purity AgI (99.999%) and AgBr (99.999%), obtained from Apache Chemicals, were used without further treatment. In some experiments, AgBr obtained from Mr. Charles B. Childs of the University of North Carolina was used. Al_2O_3 (99.98%) of varying particle sizes was obtained from Adolf Meller and was also used as received except for certain experiments in which the Al_2O_3 was vacuum-dried at ~700°C for 10–12 hr prior to use. Fumed SiO_2 of 0.007-μm diam was obtained from Cabot Corporation and used without further treatment. Fly ash of unknown purity and composition was kindly supplied by Dr. Robert Pond of Johns Hopkins University and was also used without further treatment. The size of these particles was determined, using SEM, to vary between, 0.1 and 100 μm. However, most particles were of 4- to 6-μm sizes and quite spherical.

(*ii*) *Preparation of the Samples*

Appropriate amounts of AgI and Al_2O_3 (dried or undried) were weighed and thoroughly mixed in an agate mortar and pestle, sealed under vacuum in quartz tube, heated at 600–800°C for several hours, and then quenched to room temperature, followed by pulverization and pelletization in a nickel-plated steel die at pressures of the order of 70–80 kpsi. Cylindrical pellets thus obtained were 0.71 cm^2 in area and 4–6 mm in thickness.

AgI–SiO_2 samples were prepared the same way, including premelting of the electrolytes, except that SiO_2 was used without any drying prior to mixing with AgI.

Fly ash was also used without predrying and the AgI–fly ash mixtures were pulverized and pelletized directly without undergoing the process of sealing in a quartz tube and melting the mixture, because these latter processes generally resulted in a somewhat lower enhancement of conductivity, as discussed later.

AgI–AgBr samples were prepared by melting (at ~ 600°C) the appropriate amounts of AgI and AgBr together, shaking the melt a number of times to ensure the homogeneity of the samples, followed by quenching to room temperature, pulverization, and then pelletization at pressures of the order of 70–80 kpsi.

(*iii*) *Measurement Technique*

The cylindrical pellets with an area of 0.71 cm^2 and thicknesses of 4 to 6 mm and whose parallel faces were coated with high-purity silver paint (Structure Probe, Inc.) were mechanically sandwiched between two electrodes of silver sheet to form the cells of the type.

(Ag)|Ag–paint|AgI or (AgI + dispersoids)|Ag–paint|(Ag) were used to measure the total (ac) conductivity. Since these materials generally exhibit extremely low electronic (or hole) conductivity, the measured ac (or total) conductivity is essentially the ionic conductivity of these materials. Further details regarding the impedance meter, its supplemental special-purpose generator and a matching null point detector, the furnaces, and the temperature control and measurement systems are described elsewhere (*8*).

Results and Discussion

(*i*) *Characterization Studies*

Because of the complex behavior of the samples containing dispersion of Al_2O_3, as well as others, it seemed extremely important to undertake extensive and careful characterization studies, which included the determination of surface area to find the correct particle sizes, thermogravimetric (TGA) and differential thermal analysis (DTA), differential scanning calorimetry (DSC), moisture adsorption/desorption studies, scanning electron microscopy (SEM), and X-ray diffraction studies to determine the crystallinity and/or the solubility of one phase into the other. Some of these studies, specifically TGA, DTA, and DSC, are thus far limited to the AgI–Al_2O_3 system, and were kindly carried out by the scientific staff at TRW (*14*).

Surface area determinations showed that as the particle size of Al_2O_3 decreases, the surface area increases as expected. For example, the 8-μm size Al_2O_3 has a surface area of less than 1 m^2/g. Drying the sample at 700°C has no effect on the surface area of 8- and 0.06-μm samples. Slight decreases in the surface area were detected for the 3-, 1-, and 0.3-μm Al_2O_3 samples.

No detectable weight loss was observed by TGA for the as-received 8-, 3-, and 1-μm-size Al_2O_3 samples upon heating the sample to 800°C. The 0.3-μm-size Al_2O_3 lost about 1% by weight and the 0.06-μm sample exhibited a 5% weight loss. Water adsorption studies yielded confirmatory results. The 8-, 3-, 1-, and 0.3-μm size Al_2O_3 samples did not adsorb a detectable quantity of water when exposed to a moist atmosphere (30% relative humidity) after drying at 700°C. The 0.06-μm-size Al_2O_3 adsorbed ~2% by weight when exposed to the same moist environment. It was concluded that water adsorption/desorption characteristics of the Al_2O_3 samples are related to the type (α or γ) of Al_2O_3 present in the sample. The 8-, 3-, and 1-μm samples are all α-Al_2O_3, which seems to be very resistant to hydration. The 0.3-μm sample is largely γ-Al_2O, but also contains some α-Al_2O_3, and the 0.06-μm sample consists of only γ-Al_2O_3, which readily takes up water.

Heat treatment of the Al_2O_3 has a definite effect on the thermal characteristics of AgI–Al_2O_3 specimens. Samples that contain dried Al_2O_3 have very sharp peaks in the thermograms. Samples containing undried Al_2O_3 exhibit additional thermal peaks, and many of them are diffuse and broad, particularly the melting point endotherm and the crystallization exotherm.

Electron micrographs (5,000 and 10,000×) of the samples containing dried and undried Al_2O_3 did not show any perceptible change in the surface structure. The 8-μm sample is composed of large nonporous particles and the 3-μm sample contains larger particles than the 8-μm sample but they are porous. The other samples, 1-, 0.3-, and 0.06-μm Al_2O_3, contain many agglomerates of small particles.

The fly ash sample consists of particles varying in size from 0.1 to 100 μm, but the average particle size lies somewhere between 4 and 6 μm. One marked difference between fly ash and Al_2O_3 particles was that the fly ash particles were surprisingly spherical.

X-ray diffraction studies on AgI–AgBr samples revealed that hexagonal (wurtzite) AgI can dissolve only small amounts (4 to 5 mole%) [m/o] of AgBr at room temperature (25°C). On the other hand, NaCl-type AgBr dissolves as much as ~30 (m/o) AgI at 25°C. However, the maximum conductivity is obtained for the composition AgI(80 m/o)–AgBr(20 m/o), i.e., AgI-rich region, which means the two-phase mixture. Of course, this is not a mixture of pure AgI or AgBr but of AgI saturated with (5 m/o) bromine and AgBr saturated with (~30 m/o) iodine.

(ii) Electrical Conductivity vs Composition

(a) AgI–Al_2O_3. Figure 1 shows the logarithm of ac conductivity (log σ) as a function of the composition at room temperature for the AgI–Al_2O_3 system, containing both dried and undried (as received) Al_2O_3 particles of 0.06-μm size, as well as dried ones of 0.3- and 8-μm sizes (*8*). The conductivity of the AgI–Al_2O_3 system increases initially with the increasing content of Al_2O_3, for both dried and undried and for all sizes of Al_2O_3 particles. The conductivity peaks around 30 m/o Al_2O_3 content and then decreases. The dispersion of undried Al_2O_3 of 0.06-μm size leads to a relatively sharp maximum as well as to more conductivity enhancement than the predried Al_2O_3. This latter result indicates the possibility that the presence of adsorbed water on the Al_2O_3 particles plays an important role in enhancing the conductivity. A maximum conductivity of $\sim 6 \times 10^{-4}$ ohm^{-1} cm^{-1} at room temperature was obtained for AgI containing 30 m/o undried Al_2O_3 (0.06 μm). Furthermore it is clear from Fig. 1 that the conductivity enhancement is a strong function of the size of the dispersed particles. The conductivity of AgI + 30 m/o Al_2O_3 (0.3 μm) is, for example, lower by a factor of 7 than that of AgI + 30 m/o Al_2O_3 (0.06 μm) at room temperature. When Al_2O_3 particles as large as 1 μm or more are dispersed, there is very little or practically no enhancement in conductivity, which is in qualitative agreement with a recent theoretical model (*7*) that predicts

$$\Delta\sigma \alpha \lambda \left(\frac{1}{r_1}\right) \frac{V_v}{1 - V_v}, \qquad (1)$$

where $\Delta\sigma$ is the enhancement in conductivity of the matrix by the dispersoid, λ the thickness of the space charge layer ($\sim$ Debye length), r_1 the radius (half the size) of the dispersed particles, and V_v the volume fraction of the dispersoids. Thus the enhancement is inversely proportional to the radius of the dispersoids (r_1) and directly proportional to $V_v/(1 - V_v)$ in qualitative agreement with experiments. This model, however, applies when the concentration (number per cm^3) of the dispersoids is fairly low, i.e., when the distance between two dispersoids $r_2 \gg r_1$, and therefore does not predict a maximum and the subsequent fall-off in the conductivity at higher concentrations of the dispersoids. These and other unexplained features, together with the electronic (hole) conductivity and thermoelectric properties of AgI (Al_2O_3), are discussed in greater detail elsewhere (*8*). The previous studies are thus far limited only to inclusion of Al_2O_3 in different matrices (e.g., LiI, AgI, CuCl, etc.), with one exception (*10*) that deals with LiI–SiO_2.

Here we shall focus our attention on the effects of different dispersoids (e.g., Al_2O_3, SiO, fly ash, AgBr) in the same matrix (AgI).

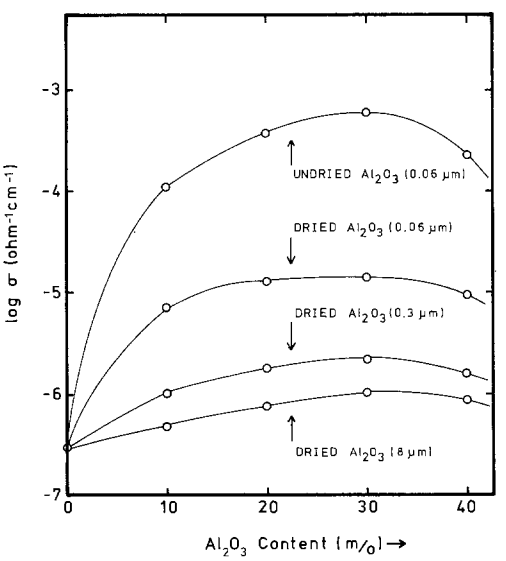

FIG. 1. Logarithm of conductivity (log σ) of the AgI–Al_2O_3 system as a function of Al_2O_3 content at 25°C for samples annealed below T_c. Note the large enhancement due to undried Al_2O_3 (0.06 μm) particles and very little enhancement due to large size (8 μm, dried or undried) Al_2O_3 particles (*8*).

(*b*) *AgI–fly ash.* AgI–fly ash samples behave somewhat differently from AgI–Al_2O_3 (or SiO_2). In this system, the maximum enhancement in σ is obtained for the samples which contain undried fly ash, similar to AgI–Al_2O_3, and the mixture has not been melted prior to pelletization (unlike AgI–Al_2O_3). AgI samples containing fly ash that had been vacuum-dried at ~600°C for 12 hr prior to mixing with AgI exhibited σ 2–3 times lower than those of AgI + (undried) fly ash samples. It was also noted that premelting of these samples, AgI + fly ash (dried or undried), prior to pelletization further decreased the conductivity by a factor varying between 2 and 4. These observations further strengthen the notion (*8*) that the presence of water in one way or the other does lead to more enhancement. However, the precise reason for the difference between the premelted AgI–Al_2O_3 and AgI–fly ash samples is unknown at present, but it is likely that any heat treatment (predrying or premelting) of the fly ash changes the surface states of the particles, therefore reducing the enhancement in σ. One such possibility, for example, could be that during the course of heating the smaller particles form larger aggregates leading to reduced surface area and hence less enhancement in the σ. On the other hand, in the AgI–Al_2O_3 (or SiO_2) system, premelting the mixtures at 600–800°C led to a somewhat higher enhancement in σ possibly because these temperatures (600–800°C) are not high enough to allow for sintering and/or forming agglomerates, as further evidenced by SEM examinations (to be discussed later) of the premelted and unmelted samples of AgI–Al_2O_3 which revealed no appreciable change in the particle size of the dispersoids in the two samples.

Another striking difference between the AgI–Al_2O_3 and AgI–fly ash systems is that the dispersion of (dried or undried) fly ash particles of ~5 μm causes significant enhancement. The reason is not known. It should be very interesting to study the dependence of enhancement on the particle size of the fly ash. Unfortunately, we cannot do it at the moment as the fly ash samples of different sizes are unavailable.

Figure 2 shows the log σ vs composition plot for the AgI–fly ash system at two different temperatures (24 and 80°C). In this and the subsequent studies, the samples used are the ones that yield optimum enhancement, i.e., AgI + undried fly ash pellitized without premelting the mixture. Since we do not know the exact chemical composition of the fly ash used, log σ is plotted against weight% (w/o) rather than (m/o) of fly ash. The qualitative features and the shapes of these curves are much the same as those in Fig. 1 for AgI–Al_2O_3 systems, viz., the conductivity increases with increasing fly ash concentration, peaks around 13.5 w/o, and then decreases. There are, however, some notable differences. First, the rise in conductivity (Fig. 2) is extremely sharp near the vi-

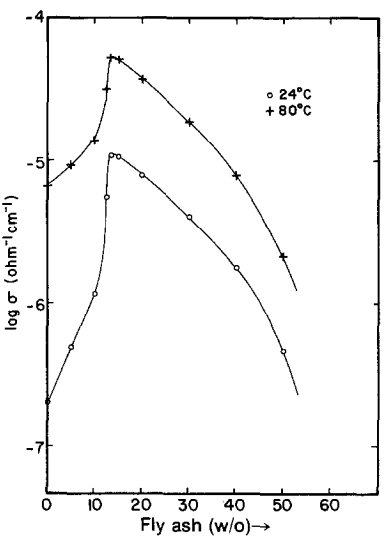

FIG. 2. Log σ as a function of fly ash (4 to 6 μm) content (weight%) in AgI at 24 and 80°C. Note the sharp rise in conductivity in the vicinity of the maximum and also the fact that the same-size Al_2O_3 particles (dried or undried, Fig. 1) lead to a relatively negligible enhancement in σ (*13*).

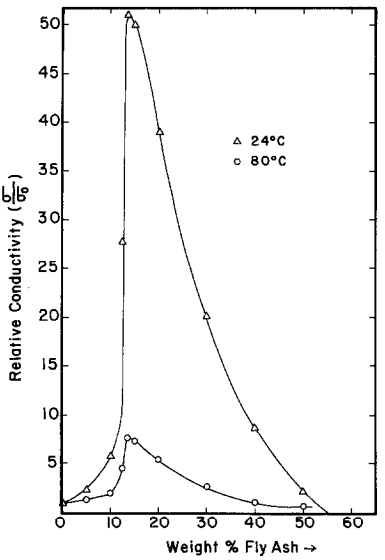

FIG. 3. Relative conductivity, σ/σ_0, where σ is the conductivity of AgI + fly ash and σ_0 that of pure AgI, as a function of the concentration w/o of fly ash in AgI, at 24 and 80°C. Note the pronounced peak at ~13.5 w/o fly ash as the large enhancement in σ at room temperature.

cinity of the maximum. See also Fig. 3, where relative conductivity (σ/σ_0), being the conductivity of AgI containing fly ash and σ_0 that of pure AgI, is plotted against the concentration of fly ash. Quantitatively, the inclusion of 10 w/o fly ash in AgI increases the conductivity by a factor of 5.8, while the addition of 3.5 w/o more fly ash changes the conductivity by a factor of almost 10.

Figure 4 shows the same results, viz., log σ vs composition plot for the AgI–AgBr system at room temperature. As mentioned under Experimental, although at room temperature the NaCl-type AgBr dissolves ~30 m/o AgI, which has a hexagonal (wurtzite type) structure, the solubility of the AgBr in the AgI is relatively limited to about $\leq$ 5 m/o at room temperature. The maximum in the log σ vs composition plot occurs at about 80 m/o AgI, which therefore corresponds to a two-phase mixture. The maximum room temperature conductivity is 3×10^{-4} ohm^{-1} cm^{-1}, which is almost three orders of magnitude higher than that of either pure AgI or pure AgBr. The AgI–AgBr (20 m/o) composition is, however, not a mixture of pure AgI and AgBr but of AgI saturated with bromine (~5 m/o) and AgBr saturated with iodine (~30 m/o), viz., a mixture of solid solutions of β-$AgI_{0.95}Br_{0.05}$ and $AgBr_{0.70}I_{0.30}$. Since bromide and iodide ions have the same charge (i.e., homovalent ions), the substitution of one for the other should not lead to any significant change in the ionic conductivity or related properties, but the effect is dramatic (see the solid-solution regions at the extremities in Fig. 4) and is attributed to purely elastic displacement (lattice distortion) caused by the substitution of "wrong"-size ions into the host lattice. This phenomenon is also treated in detail elsewhere (*15*).

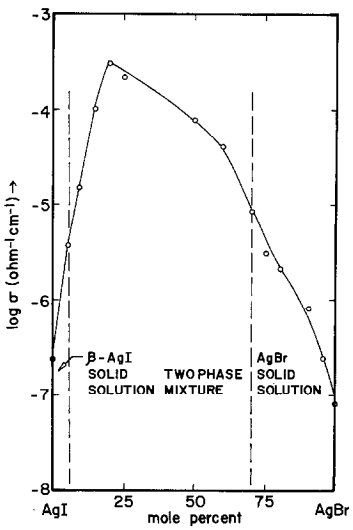

FIG. 4. Log σ of AgI–AgBr system as a function of composition at 25°C. Although NaCl-type AgBr dissolves ~30 m/o hexagonal AgI at 25°C, solubility of the former (AgBr) in the latter (β-AgI) is very limited ($\leq$ 5 m/o) and therefore the composition corresponding to the maximum in the plot consists of a two-phase mixture, β-AgI saturated with bromine (β-$AgI_{0.95}Br_{0.05}$) + AgBr saturated with iodine ($AgBr_{0.7}I_{0.3}$).

The composition [AgI–AgBr (20 m/o)] corresponding to maximum conductivity, in view of the mentioned solubilities, will actually consist of 77 m/o $AgI_{0.95}Br_{0.05}$ and 23 m/o $AgBr_{0.70}I_{0.30}$, whose individual conductivities, from Fig. 4, are 5×10^{-6} ohm^{-1} cm^{-1} and 8×10^{-6} ohm^{-1} cm^{-1}, respectively, at room temperature. This would lead to a classical average conductivity of 5.7×10^{-6} ohm^{-1} cm^{-1} for the mixture $AgI_{0.95}Br_{0.05}$ + $AgBr_{0.70}I_{0.30}$ (23 m/o), while the observed conductivity is $\sim 3 \times 10^{-4}$ ohm^{-1} cm^{-1}, i.e., higher by a factor of ~53. This figure (i.e., a σ enhancement by a factor of 53) is almost the same as that in AgI–fly ash (~51) and AgI–dried Al_2O_3 (0.06 μm) (~50), and very close to that (~45) in AgI–SiO_2 (Table I). This appears to be more than just a coincidence. See Table I for a summary of some of the characteristics of AgI containing different dispersoids, as well as those of LiI (Al_2O_3) and CuCl (Al_2O_3). Strikingly, in almost all systems the enhancement in conductivity is about a factor of 50. One exception to this generality is the AgI–undried Al_2O_3 (0.06 μm) system in which an enhancement by a factor of 10^3 is obtained. It seems appropriate here to mention that thermal analyses (such as DTA, TGA, etc.) of the AgI–Al_2O_3 system indicate that Al_2O_3 of 0.06-μm size possibly has a tendency to react with AgI and this tendency is somewhat pronounced expecially when they are "wet" (*12, 13, 15*).

(*iii*) *Electrical Conductivity vs Temperature*

Figure 5 shows the log conductivity as a function of temperature for AgI and AgI containing 30 m/o dried as well as undried Al_2O_3 of 0.06-μm size (*8*). Pure AgI has a conductivity of $\sim 2.4 \times 10^{-7}$ ohm^{-1} cm^{-1} at 25°C and an overall activation energy of 0.56 eV. AgI containing 30 m/o undried Al_2O_3 (0.06 μm) has a conductivity of $\sim 6 \times 10^{-4}$ ohm^{-1} cm^{-1} at 25°C, i.e., $\sim 10^3$ times higher than that of pure AgI at the same temperature, while the conductivity of AgI containing the same amount of the same size but dried Al_2O_3 is $\sim 1.2 \times 10^{-5}$ ohm^{-1} cm^{-1} at 25°C, which is about 50 times higher than that of pure AgI. This leads to the possibility that adsorbed water on Al_2O_3 surfaces also plays a role in enhancing the

TABLE I

SOME CHARACTERISTICS OF SOLID ELECTROLYTE AgI CONTAINING A VARIETY OF DISPERSOIDS AND THEIR COMPARISON WITH OTHER SYSTEMS

Material	Dispersoid and its size (μm)	Percentage dispersoid for maximum enhancement	Temperature (°C)	Maximum enhancement in σ by factor
AgI	Dried Al_2O_3 (0.06)	30 m/o	25	50 (this work)
AgI	SiO_2 (0.007)	10 m/o	25	45 (this work)
AgI	Fly ash (~ 4–6)	13.5 w/o	25	51 (this work)
Ag(I,Br)	Ag(Br,I) (unknown)	23 m/o	25	53 (this work)
LiI	Al_2O_3 (unknown)	40 m/o	25	~50 (Ref. 9)
CuCl	Al_2O_3 (0.06)	10 m/o	60	~50[a]

[a] Unpublished data of K. Shahi and J. B. Wagner, Jr.

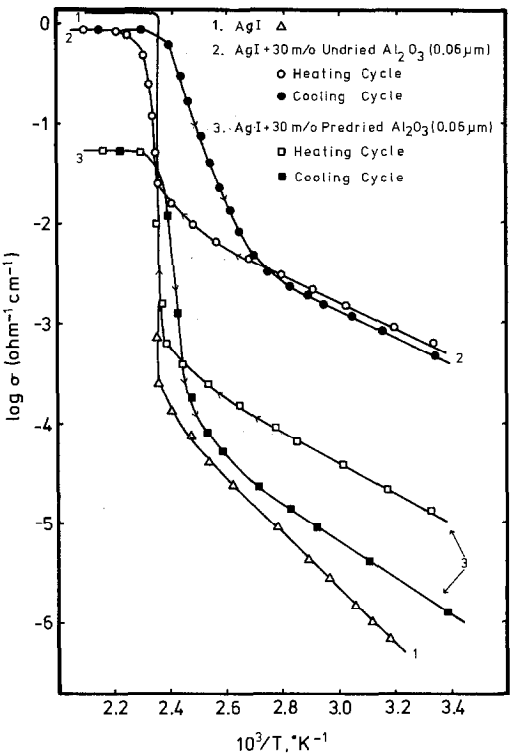

FIG. 5. Log σ of AgI and AgI containing dispersion of dried and undried Al_2O_3 (0.06 μm, 30 m/o) as a function of inverse of absolute temperature. Note that larger enhancement in σ is accompanied by a decrease in the activation energy, as well as a significant hysterisis in log σ vs temperature plot (*8*).

conductivity. Table II summarizes the room temperature conductivities and the electrical transport parameters of the Arrhenius equation

$$\sigma = \sigma_0 \exp\left(-\frac{E_a}{kT}\right), \qquad (2)$$

where σ is the conductivity, σ_0 the preexponential factor that depends, among others, upon the concentration, the attempt frequency, and the jump distance of the atomic defects, E_a the overall activation energy, k the Boltzmann constant, and T the absolute temperature (°K). It is obvious from Table II that the conductivity enhancement is invariably accompanied by a decrease in overall activation energy.

Figure 6 shows the same results, viz., log σ vs reciprocal of temperature, for AgI and AgI containing dispersion of fly ash (4–6 μm). As mentioned earlier, for AgI containing 5 and 10 w/o fly ash, the increase in conductivity is relatively small and, as expected, a little decrease in activation energy is observed (Table II).

However, for AgI + 10 w/o fly ash and AgI + 15 w/o fly ash, the enhancement in the conductivity is relatively large and is accompanied by an appreciable change in activation energy. The dispersion of fly ash, quite like that of Al_2O_3, slightly decreases the conductivity in the high-temperature α phase of AgI, which is expected in view of the exceptionally high conductivity of α-AgI. The accuracy of measurements around 1 ohm^{-1} cm^{-1} was not high enough to detect the successive changes in the conductivity of AgI containing different concentrations of fly ash, but was sufficient to reveal that

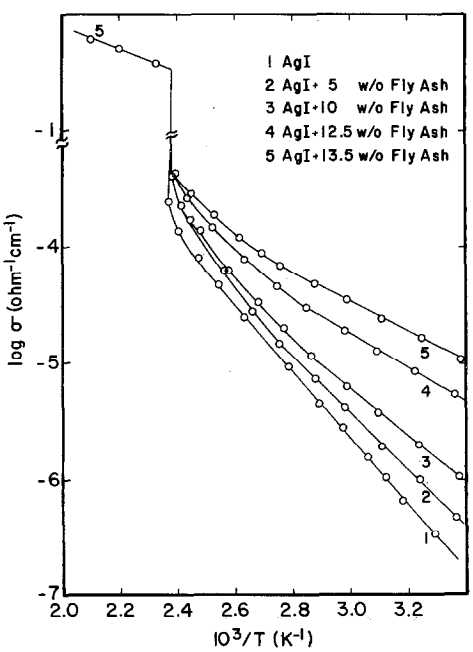

FIG. 6. Log σ of AgI containing different concentrations of fly ash (4 to 6 μm) as a function of the inverse absolute temperature.

TABLE II

SUMMARY OF ELECTRICAL TRANSPORT DATA OF SOME MULTIPHASE SYSTEMS AND/OR DISPERSED SOLID ELECTROLYTE SYSTEMS FOR THE SAMPLES ANNEALED BELOW T_c OF AgI

Material composition	σ_{RT} (ohm^{-1} cm^{-1})	σ_0 (ohm^{-1} cm^{-1})	E_a (eV)	Temp. range (°C)
AgI + 0 m/o Al_2O_3	2.4×10^{-7}	6.71×10^{2}	0.56	25–110
+ 30 m/o dried Al_2O_3 (0.06 μm)	1.2×10^{-5}	6.34×10^{-2}	0.31	25–100
+ 30 m/o undried Al_2O_3 (0.06 μm)	6×10^{-4}	1.31×10^{1}	0.26	25–100
AgI + 0 m/o SiO_2	2.4×10^{-7}	6.71×10^{2}	0.56	25–110
+ 5 m/o SiO_2 (0.007 μm)	4.2×10^{-6}	9.24×10^{-1}	0.34	25–110
+ 10 m/o SiO_2 (0.007 μm)	1.1×10^{-5}	3.32×10^{-1}	0.29	25– 85
AgI + 0 w/o fly ash	2.4×10^{-7}	6.71×10^{2}	0.56	25–110
+ 5 w/o fly ash	4.7×10^{-7}	6.57×10^{1}	0.48	25– 90
+ 10 w/o fly ash	1.1×10^{-6}	6.63×10^{0}	0.40	25– 85
+ 12.5 w/o fly ash	5.3×10^{-6}	4.30×10^{-1}	0.29	25– 80
+ 13.5 w/o fly ash	1.2×10^{-5}	2.86×10^{-1}	0.26	25– 80
AgI + 0 m/o AgBr*	2.4×10^{-7}	6.71×10^{2}	0.56	25–110
+ 1 m/o AgBr*	4.6×10^{-7}	2.83×10^{2}	0.52	25–110
+ 2 m/o AgBr*	1.5×10^{-6}	9.29×10^{1}	0.46	25–110
+ 4 m/o AgBr*	4.1×10^{-6}	2.37×10^{1}	0.40	25–100
+ 10 m/o AgBr	1.7×10^{-5}	4.29×10^{-1}	0.26	25– 85
+ 15 m/o AgBr	8.7×10^{-5}	1.46×10^{0}	0.25	25– 80
+ 20 m/o AgBr	3.2×10^{-4}	1.70×10^{0}	0.22	25– 80

Note. σ_0 refers to room temperature (RT) conductivity, and σ_0 and E_a are the parameters of the Arrhenius equation $\sigma = \sigma_0 \exp(-E_a/kT)$. The starred (*) compositions correspond to single-phase AgI solid solution.

the higher the concentration of fly ash the lower the conductivity in the α-AgI region. For that reason, Fig. 6 shows the results in α-AgI phase corresponding only to one concentration (i.e., 13.5 w/o fly ash–AgI).

Figure 7 compares the conductivities of two samples annealed above and below the transition temperature of AgI (i.e., 147°C). Samples annealed above T_c exhibit, in general, a lower conductivity than those annealed below T_c, for reasons not clearly understood. This behavior was quite common for all dispersed-AgI systems, except that of AgI–AgBr (>4 m/o), i.e., the two-phase system discussed later. Another general feature of all dispersed-AgI systems was the occurrence of hysterisis in log σ vs $10^3/T$ plots like that shown in Fig. 5 for the AgI–Al_2O_3 system. The width of the hysterisis loop was usually ~4–6°C, however, again there was an exception of AgI–undried Al_2O_3 (0.06 μm) where it was ~16°C.

Figure 8 shows the log σ vs $10^3/T$ plots for AgI containing different amounts of AgBr (*12, 15*). AgI dissolves ~5 m/o AgBr at room temperature, and therefore the compositions AgI containing 1, 2, and 4 m/o AgBr correspond to single-phase AgI : Br^- solid solutions. Thus the incorporation of Br^- ions in the iodine sublattice produces appreciable change in the ionic conductivity and also in the activation en-

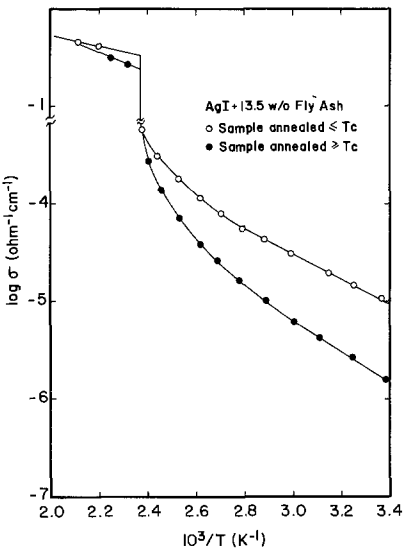

FIG. 7. Log σ vs $10^3/T$ for AgI containing 13.5 w/o fly ash. Samples annealed above T_c exhibit lower conductivities than those annealed below T_c.

ergy to some extent (Table II), as does the substitution of I^- ions in AgBr. These changes are believed to be due to purely elastic displacement of the host ions (lattice distortion), leading to loosening of the lattice and consequently to increased defect concentration and hence conductivity, and are treated separately elsewhere (*12, 15*). Nevertheless, AgI containing higher concentrations of AgBr consists of a two-phase mixture of $AgI_{0.95}Br_{0.05}$ and $AgBr_{0.70}I_{0.30}$ rather than of pure AgI and AgBr, and, as can be seen in Fig. 8, the conductivity enhancement in the two-phase region is even more dramatic. The effect of a two-phase mixture on the activation energies is also clearly noticeable. For instance, AgI + 4 m/o AgBr has an $E_a \sim 0.40$ eV compared to 0.26 eV for the two-phase mixture AgI + 10 m/o AgBr (see Table II).

The effect of substitution of Br^- in α-AgI region ($>T_c$) is possibly to decrease the conductivity, at least in the investigated temperature range. For clarity, only the results on pure AgI and AgI + 20 m/o AgBr are shown in the high-temperature (α) phase (Fig. 8). It is also interesting to note in this figure that the $\beta \rightarrow \alpha$ phase transition temperature (T_c) is decreasing with increasing concentration of AgBr in AgI (or dissolved Br^- ions in AgI) until it is saturated (about 9–10 m/o at 128°C), and therefore there is no change in T_c with further addition ($\geq$10 m/o) of AgBr in AgI. The T_c decreases almost linearly with the substituted Br^- ion concentration, at the rate of about 2°C per m/o of added AgBr. It is believed that the first-order transition in AgI is essentially driven by a critical concentration of Frenkel defects. When the critical concentration of the defects is attained, the hexagonal AgI is no longer able to sustain its structure and transforms to cubic α-AgI. By substituting Br^- in AgI, the

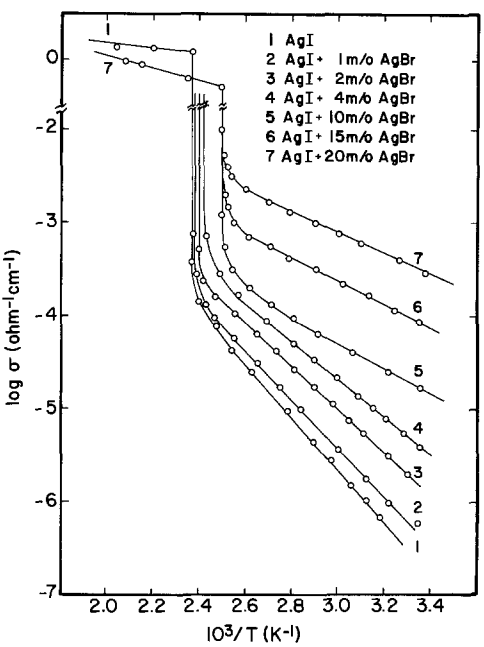

FIG. 8. Log σ vs $10^3/T$ for AgI containing various amounts of AgBr (*12*). Essential features are the same as in Figs. 5–7 except that, since AgI dissolves AgBr to some extent (~10 m/o at 128°C), there is a gradual decrease in the β–α phase transition temperature (T_c) of AgI with increasing concentration of AgBr. A detailed discussion of T_c vs Br concentration in AgI and its analogy with that of hydrostatic pressure is available elsewhere (*15*).

conductivity and hence the defect concentration (or thermal disorder) is increased and accordingly the critical concentration is attained at a relatively low temperature, i.e., lower T_c. A further discussion of T_c and the factors influencing T_c is beyond the scope of this paper and is treated elsewhere (*16*).

(iv) Microstructure and the Frequency-Dependent Conductivity

Because of the nature of materials (high surface area) involved, one obvious question often raised is whether or not the enhancement in conductivity is due to grain-boundary or surface conduction. To answer this question, numerous samples, especially of AgI–Al_2O_3 and AgI–fly ash, have been examined with the help of a scanning electron microscope (SEM) that was fitted with an EDX chemical analyzer. Despite the high concentration (~30 m/o) of Al_2O_3 of 0.06-μm size in AgI, it was quite difficult to locate very many Al_2O_3 particles in the premelted samples of AgI–Al_2O_3, possibly because of the fact that in such premelted samples, each Al_2O_3 particle is coated with a thick layer of AgI rendering the Al_2O_3 surface unexposed. On the other hand, no such difficulty was encountered when the sample under examination was prepared without melting the mixture. The observed sizes of Al_2O_3 particles were found to be somewhat different from those quoted by the supplier (Adolf Meller) and also many of the particles are nonsperical. For instance, the examination of electron micrographs of AgI + 8-μm Al_2O_3 showed that the particles vary in size from 5 to 20 μm and contain no porosity, and that no change occurs on drying. On the other hand, the micrographs of AgI + 0.06-μm Al_2O_3 showed that particles are much smaller ($\leq$0.01 μm) and some larger agglomerates similar to those in AgI + 0.3-μm Al_2O_3 and AgI + 1-μm Al_2O_3 specimens are present. The fact that 0.06-μm Al_2O_3 particles are much smaller ($\leq$0.01 μm), combined with their uniqueness of adsorbing water quickly, possibly explains the substantially higher enhancement in conductivity caused by their dispersion. In general, it was noted that the dried samples have a little more tendency to agglomerate (reduced surface area) than the undried ones, which partly accounts for the lower conductivity enhancements by the former as compared to the latter ones.

Fly ash samples are somewhat different. First, most of the particles were found to be surprisingly spherical (see Fig. 9). Second, some of them are porous and contain holes on their surfaces (Fig. 10), and lastly, some particles as small as 0.1 μm and as large as 100 μm were present, but the average particle size was, however, estimated to be 4 to 6 μm. The dispersion of these particles led to an enhancement by a factor of $\geq$50, while the equivalent-size Al_2O_3 particles had no appreciable effect.

The high-magnification micrographs of pure AgI and AgI containing dispersions revealed that the dispersions of Al_2O_3 or fly ash have little effect on the grain size (~10–20 μm) of the samples and therefore it is

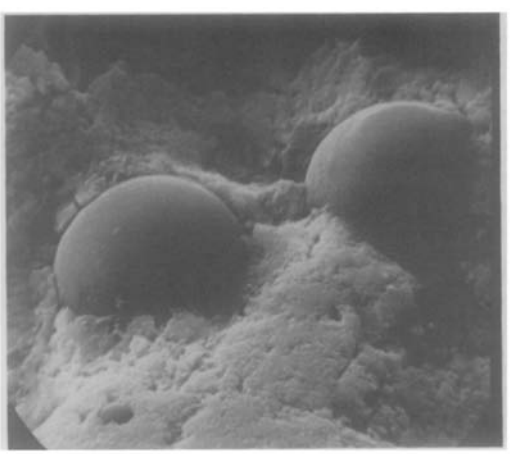

FIG. 9. Electron micrograph (3200×) of an AgI–fly ash sample. Two large fly ash particles (approx diam 10 μm) are embedded in AgI matrix and are very spherical in shape.

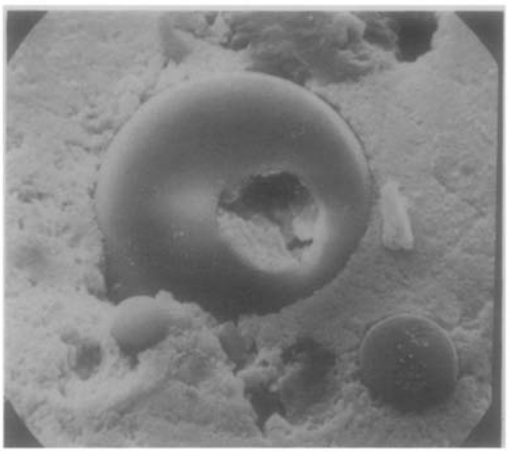

FIG. 10. Electron micrograph (1800×) of AgI sample containing a dispersion of fly ash particles. Note again the surprisingly spherical shape of the particles. A few of them have holes on their surfaces; one seen above is as large as ~11 μm in diam.

believed that the grain-boundary or surface conduction is less likely to be the mechanism of enhancement.

These data were further supplemented by the measurement of conductivity on pure and dispersed AgI as a function of frequency at different temperatures. The presence of substantial grain-boundary conduction is expected to exhibit a significant frequency-dependent conductivity. Figure 11 shows a typical plot of conductivity normalized to that at 1 kHz ($\sigma/\sigma_{1\ \mathrm{kHz}}$) in order to facilitate the comparison of the data at various temperatures as a function of the logarithm of frequency at three different temperatures for AgI–fly ash (13.5 w/o). Obviously there is very nominal frequency dependence at all temperatures. For example, the conductivity at 50 kHz is only ~25% higher than that at 50 Hz for all three temperatures, very similar to that for AgI–Al_2O_3. Furthermore, the pure AgI without any dispersion behaves more or less the same way and some of the data points would fall on the same curve (Fig. 11) if plotted. For reasons of clarity, the data on AgI and AgI (Al_2O_3) are not shown in Fig. 11. It is thus concluded that the enhanced conductivity in the dispersed solid electrolyte is due to the bulk rather than the grain-boundary or surface conduction.

Summary

Ionic conductivity measurements of AgI containing a variety of dispersions, e.g., Al_2O_3, SiO_2, fly ash, etc., as well as such two-phase mixtures as AgI–AgBr, were carried out as a function of composition, temperature, and frequency. Although in certain cases, for instance, AgI–undried Al_2O_3, conductivity enhancements of up to 3 orders of magnitude were obtained, it seems that enhancement is generally limited to a factor of 50 (or 1.7 orders of magnitude) at room temperature. While the enhancement strongly depends on the size of the particles dispersed, the same-size particles of various materials (Al_2O_3, SiO, fly ash, etc.) seem to yield different degrees of enhancement in σ. The high-amplification (3,000 to 10,000×) electron micrographs, as well as the frequency-dependent conductiv-

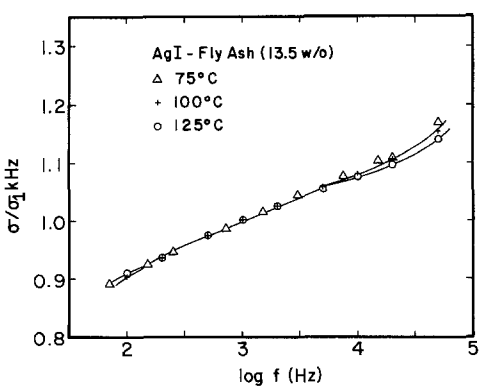

FIG. 11. The conductivity (σ) normalized to that at 1 kHz ($\sigma_{1\ \mathrm{kHz}}$) of AgI containing 13.5 w/o fly ash as a function of the frequency at three different temperatures. Frequency dependence is obviously very nominal (~ 25% between 50 Hz and 50 kHz) and more significantly is the same as that of pure AgI, as well as at all temperatures, indicating that enhancement in σ is unlikely to be due to increased surface or grain-boundary conduction.

ity data, indicate that the enhancement is due to bulk rather than grain-boundary or surface conduction. Furthermore, the conductivity and the thermoelectric power data suggest that fine dispersoids generate an excess of lattice defects (e.g., Ag^+ ion vacancies in $AgI–Al_2O_3$) and thereby enhance the conductivity, which is consistent with a recent theoretical model.

Acknowledgment

This research was supported by NASA Contract NAS8-32937.

References

1. P. VASHISHTA, J. N. MUNDY, AND G. K. SHENOY (Eds.), "Fast Ion Transport: Electrodes and Electrolytes," North-Holland, Amsterdam (1979).
2. "Solid State Ionics," Proceedings, 3rd International Conference on Solid Electrolytes, Tokyo, Sept. 1980, North-Holland, Amsterdam, to be published.
3. B. B. OWENS AND G. R. ARGUE, *Science* **157,** 308 (1967).
4. Y. YAO AND J. T. KUMMER, *J. Inorg. Nucl. Chem.* **29,** 2453 (1967).
5. A. AVOGADRO, S. MANZINI, AND M. VILLA, *Phys. Rev. Lett.* **44,** 256 (1980); see also J. P. MALUGANI, A. WASNIEWSKI, M. DOREAU, AND G. ROBERT, *Mater. Res. Bull.* **13,** 427 (1978).
6. C. C. LIANG, *J. Electrochem. Soc.* **120,** 1289 (1973); see also C. C. LIANG, A. V. JOSHI, AND N. E. HAMILTON, *J. Appl. Electrochem.* **8,** 445 (1978).
7. T. JOW AND J. B. WAGNER, JR., *J. Electrochem. Soc.* **126,** 1963 (1979).
8. K. SHAHI AND J. B. WAGNER, JR., *J. Electrochem. Soc.* **128,** 6 (1981).
9. S. PACK, B. B. OWENS, AND J. B. WAGNER, JR., *J. Electrochem. Soc.* **127,** 2177 (1980).
10. P. M. SKARSTAD, D. R. MERRITT, AND B. B. OWENS, Extended abstract *in* "Solid State Ionics," Proceedings, 3rd International Conference on Solid Electrolytes, Tokyo, Sept. 1980, North-Holland, Amsterdam, to be published.
11. A. M. STONEHAM, E. WADE, AND J. A. KILNER, *Mater. Res. Bull.* **14,** 661 (1979).
12. K. SHAHI AND J. B. WAGNER, JR., *Appl. Phys. Lett.* **37,** 757 (1980).
13. A brief mention of these systems appeared in K. SHAHI AND J. B. WAGNER, JR., *Solid State Ionics* **3/4,** 295 (1981).
14. TRW Report prepared for Attached Shuttle Payloads Organization–Materials Processing in Space, NASA, Dec. 1979.
15. K. SHAHI AND J. B. WAGNER, JR., *J. Phys. Chem. Solids,* in press.
16. K. SHAHI AND J. B. WAGNER, JR., *Phys. Rev. B* **23,** 6417 (1981).